Exploratory Study of Gastrointestinal Redox Biomarkers in the Presymptomatic and Symptomatic Tg2576 Mouse Model of Familial Alzheimer's Disease: Phenotypic Correlates and Effects of Chronic Oral d-Galactose

Homolak, Jan; Babić Perhoč, Ana; Knezović, Ana; Osmanović Barilar, Jelena; Virag, Davor; Šalković-Petrišić, Melita

Source / Izvornik: **ACS Chemical Neuroscience, 2023, 14, 4013 - 4025**

Journal article, Published version
Rad u časopisu, Objavljena verzija rada (izdavačev PDF)

https://doi.org/10.1021/acschemneuro.3c00495

Permanent link / Trajna poveznica: https://urn.nsk.hr/urn:nbn:hr:105:023423

ACS Chemical Neuroscience

pubs.acs.org/chemneuro

Research Article

Exploratory Study of Gastrointestinal Redox Biomarkers in the Presymptomatic and Symptomatic Tg2576 Mouse Model of Familial Alzheimer's Disease: Phenotypic Correlates and Effects of Chronic Oral D-Galactose

Jan Homolak,* Ana Babic Perhoc, Ana Knezovic, Jelena Osmanovic Barilar, Davor Virag, and Melita Salkovic-Petrisic

Cite This: ACS Chem. Neurosci. 2023, 14, 4013–4025

Read Online

ACCESS | Metrics & More | Article Recommendations | Supporting Information

ABSTRACT: The gut might play an important role in the etiopathogenesis of Alzheimer's disease (AD) as gastrointestinal alterations often precede the development of neuropathological changes in the brain and correlate with disease progression in animal models. The gut has an immense capacity to generate free radicals whose role in the etiopathogenesis of AD is well-known; however, it remains to be clarified whether gastrointestinal redox homeostasis is associated with the development of AD. The aim was to (i) examine gastrointestinal redox homeostasis in the presymptomatic and symptomatic Tg2576 mouse model of AD; (ii) investigate the effects of oral D-galactose previously shown to alleviate cognitive deficits and metabolic changes in animal models of AD and reduce gastrointestinal oxidative stress; and (iii) investigate the association between gastrointestinal redox biomarkers and behavioral alterations in Tg2576 mice. In the presymptomatic stage, Tg2576 mice displayed an increased gastrointestinal electrophilic tone, characterized by higher lipid peroxidation and elevated Mn/Fe-SOD activity. In the symptomatic stage, these alterations are rectified, but the total antioxidant capacity is decreased. Chronic oral D-galactose increased the antioxidant capacity and reduced lipid peroxidation in the Tg2576 but had the opposite effects in the wild-type animals. The total antioxidant capacity of the gastrointestinal tract was associated with greater spatial memory. Gut redox homeostasis might be involved in the development and progression of AD pathophysiology and should be further explored in this context.

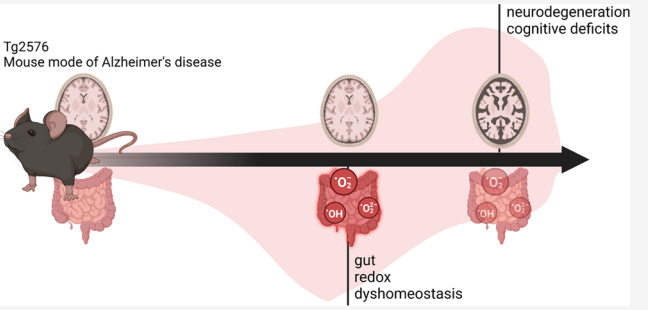

KEYWORDS: *Alzheimer's disease, gastrointestinal, gut−brain axis, redox, galactose*

INTRODUCTION

Accumulating evidence suggests that the gut might play an important role in the etiopathogenesis and progression of Alzheimer's disease (AD).[1,2] Gastrointestinal (GI) alterations have been reported in both transgenic[3−7] and nontransgenic animal models of AD.[8−11] Importantly, GI alterations often precede neuropathological changes in the brain and correlate with disease progression,[4,6] suggesting that pathophysiological processes in the gut might contribute to dyshomeostasis in the central nervous system (CNS) in the early stages of neurodegeneration. Honarpisheh et al. reported that GI dysfunction takes place before the onset of cognitive symptoms and the accumulation of cerebral amyloid-β (Aβ) in the (6 months old) Tg2576 mouse model of familial AD.[4] Similarly, pathophysiological alterations in the GI tract have been observed in the presymptomatic stage in other animal models of familial AD (e.g., TgCRND8[6] and APP/PS1[3]). Mechanisms by which gut dyshomeostasis might incite neurodegeneration are still not clear; however, current working models suggest that dysfunction of the GI barrier might promote chronic inflammation and metabolic dyshomeostasis associated with microglial activation and brain insulin resistance as key etiopathogenetic clusters of AD.[12−16] GI redox dyshomeostasis might be another mechanism by which gut dysfunction impels neurodegenerative processes: (i) oxidative stress is closely related to most molecular mechanisms driving AD;[17,18] (ii) the gut has an immense capacity to generate free radicals with detrimental health consequences[19−21] and 40% of body energy expenditure is required for the maintenance of the GI barrier, which is constantly and inevitably exposed to xenobiotics and

Received: July 22, 2023
Revised: October 26, 2023
Accepted: October 26, 2023
Published: November 6, 2023

Table 1. Gastrointestinal Redox Biomarkers in the Presymptomatic (7 Months Old) and Symptomatic (12 Months Old) Tg2576 Mice

age (months)	redox biomarker	group	estimate (CI)	contrast: ratio [p-value]
7	δABTS absorbance[a]	wt	0.54 (0.47−0.61)	
		wt + gal	0.54 (0.48−0.61)	
		tg	0.54 (0.48−0.61)	
		tg + gal	0.53 (0.46−0.60)	
12	δABTS absorbance[a]	wt	0.42 (0.38−0.54)	
		wt + gal	0.46 (0.38−0.54)	
		tg	0.43 (0.36−0.51)	
		tg + gal	0.44 (0.37−0.52)	
7	δH_2O_2 [mM][b]	wt	8.12 (6.36−9.87)	
		wt + gal	6.10 (4.55−7.65)	
		tg	7.66 (6.16−9.17)	
		tg + gal	7.38 (5.71−9.04)	
12	δH_2O_2 [mM][b]	wt	7.12 (5.68−8.55)	tg/tg + gal: 1.28 [0.049]
		wt + gal	6.94 (5.63−8.26)	tg/wt: 1.22 [0.099]
		tg	8.68 (7.43−9.93)	
		tg + gal	6.77 (5.46−8.09)	
7	CAT: δH_2O_2 [mM][c]	wt	7.91 (6.25−9.58)	tg + gal/wt + gal: 1.32 [0.085]
		wt + gal	5.84 (4.35−7.32)	wt/wt + gal: 1.36 [0.083]
		tg	7.81 (6.39−9.22)	
		tg + gal	7.70 (6.10−9.31)	
12	CAT: δH_2O_2 [mM][c]	wt	7.08 (5.59−8.57)	tg/tg + gal: 1.28 [0.055]
		wt + gal	6.93 (5.58−8.28)	
		tg	8.71 (7.41−10.01)	
		tg + gal	6.80 (5.43−8.16)	
7	GSH [μM/mL][a]	wt	13.1 (11.9−14.4)	tg + gal/wt + gal: 0.89 [0.061] (th:gen p = 0.082)
		wt + gal	13.7 (12.6−14.8)	
		tg	13.6 (12.5−14.6)	
		tg + gal	12.2 (11.1−13.4)	
12	GSH [μM/mL][a]	wt	13.4 (11.6−15.3)	tg + gal/wt + gal: 1.16 [0.068]
		wt + gal	13.1 (11.4−14.8)	
		tg	14.1 (12.5−15.8)	
		tg + gal	15.2 (13.5−16.9)	
7	H_2O_2 [mM][a]	wt	1.55 (0.93−2.12)	
		wt + gal	1.96 (1.42−2.50)	
		tg	1.78 (1.25−2.32)	
		tg + gal	1.78 (1.19−2.37)	
12	H_2O_2 [mM][a]	wt	−0.43 (−2.20−1.35)	
		wt + gal	−0.49 (−2.12−1.14)	
		tg	−0.85 (−2.39−0.71)	
		tg + gal	−0.68 (−2.32−0.95)	
7	NRP [integrated density][a]	wt	29.71×10^3 ($22.44 \times 10^3 - 36.99 \times 10^3$)	
		wt + gal	27.79×10^3 ($21.37 \times 10^3 - 36.99 \times 10^3$)	
		tg	34.77×10^3 ($28.45 \times 10^3 - 41.08 \times 10^3$)	
		tg + gal	35.03×10^3 ($28.04 \times 10^3 - 42.02 \times 10^3$)	
12	NRP [integrated density][a]	wt	42.15×10^3 ($31.19 \times 10^3 - 53.11 \times 10^3$)	tg/wt: 0.65 [0.048]
		wt + gal	32.46×10^3 ($22.41 \times 10^3 - 42.50 \times 10^3$)	
		tg	27.60×10^3 ($18.04 \times 10^3 - 37.16 \times 10^3$)	
		tg + gal	31.03×10^3 ($20.94 \times 10^3 - 41.12 \times 10^3$)	
7	ORAC [δRFU][a]	wt	1007 (470−1545)	
		wt + gal	907 (433−1381)	
		tg	1140 (674−1606)	
		tg + gal	1193 (677−1709)	
12	ORAC [δRFU][a]	wt	1020 (351−1689)	
		wt + gal	1783 (1170−2396)	
		tg	1436 (852−2019)	
		tg + gal	1304 (688−1919)	
7	PER: δH_2O_2 [mM][b]	wt	−0.01 (−0.52−1.02)	tg + gal/wt + gal: 0.42 [0.053]
		wt + gal	0.09 (−0.42−1.06)	
		tg	−0.26 (−0.60−0.36)	
		tg + gal	−0.54 (−0.77 − −0.09)	

https://doi.org/10.1021/acschemneuro.3c00495
ACS Chem. Neurosci. 2023, 14, 4013−4025

Table 1. continued

age (months)	redox biomarker	group	estimate (CI)	contrast: ratio [p-value]
12	PER: δH_2O_2 [mM][b]	wt	−4.27 (−5.29 − −2.09)	
		wt + gal	−3.52 (−4.86 − −0.85)	
		tg	−2.82 (−4.45−0.36)	
		tg + gal	−3.26 (−4.74 − −0.30)	
7	SH [μM/ml][a]	wt	16.9 (15.1−18.7)	
		wt + gal	16.2 (14.6−17.8)	
		tg	17.2 (15.7−18.8)	
		tg + gal	17.6 (15.8−19.3)	
12	SH [μM/ml][a]	wt	17.3 (15.5−19.0)	
		wt + gal	18.4 (16.9−20.0)	
		tg	16.9 (15.3−18.4)	
		tg + gal	16.7 (15.4−18.3)	
7	SOD [δTHB abs][a]	wt	0.060 (0.050−0.071)	
		wt + gal	0.057 (0.048−0.067)	
		tg	0.056 (0.047−0.065)	
		tg + gal	0.051 (0.041−0.062)	
12	SOD [δTHB abs][a]	wt	0.059 (0.050−0.067)	
		wt + gal	0.052 (0.044−0.061)	
		tg	0.056 (0.048−0.064)	
		tg + gal	0.056 (0.048−0.064)	
7	Mn/Fe-SOD [δTHB abs][a]	wt	0.058 (0.053−0.064)	
		wt + gal	0.054 (0.049−0.059)	
		tg	0.053 (0.048−0.058)	
		tg + gal	0.052 (0.046−0.057)	
12	Mn/Fe-SOD [δTHB abs][a]	wt	0.056 (0.050−0.062)	
		wt + gal	0.056 (0.051−0.062)	
		tg	0.054 (0.049−0.060)	
		tg + gal	0.056 (0.051−0.062)	
7	Mn-SOD [δTHB abs][a]	wt	0.109 (0.102−0.116)	tg/wt: 0.86 [0.004]
		wt + gal	0.095 (0.088−0.101)	
		tg	0.094 (0.088−0.101)	wt/wt + gal: 1.15 [0.009] (th:gen p = 0.077)
		tg + gal	0.091 (0.084−0.098)	
12	Mn-SOD [δTHB abs][a]	wt	0.103 (0.085−0.121)	
		wt + gal	0.118 (0.101−0.134)	
		tg	0.113 (0.098−0.129)	
		tg + gal	0.120 (0.104−0.137)	
7	Cu/Zn-SOD [δTHB abs][d]	wt	0.058 (0.047−0.068)	
		wt + gal	0.057 (0.048−0.066)	
		tg	0.057 (0.048−0.066)	
		tg + gal	0.053 (0.043−0.063)	
12	Cu/Zn-SOD [δTHB abs][d]	wt	0.058 (0.051−0.065)	
		wt + gal	0.052 (0.045−0.059)	
		tg	0.057 (0.051−0.064)	
		tg + gal	0.055 (0.049−0.062)	
7	TBARS [μM][a]	wt	9.01 (4.68−17.31)	
		wt + gal	10.53 (5.91−18.77)	
		tg	14.31 (8.11−25.26)	
		tg + gal	13.53 (1.98−3.23)	
12	TBARS [μM][a]	wt	16.85 (12.35−23.00)	tg + gal/wt + gal: 0.69 [0.060]
		wt + gal	20.95 (15.76−27.85)	
		tg	14.65 (11.18−19.21)	
		tg + gal	14.46 (10.86−19.24)	

[a]Adjusted for total protein concentration. [b]Adjusted for total protein concentration and baseline H_2O_2 concentration; δH_2O_2 is negative due to artifactual absorbance shift (low accuracy, high precision)—values do not faithfully reflect absolute numbers but enable reliable group comparisons. [c]Catalase activity was estimated from total H_2O_2 dissociation capacity adjusted for baseline H_2O_2, protein concentration, and residual activity of peroxidases. [d]Cu/Zn-SOD activity was estimated from total SOD activity adjusted for Mn/Fe-SOD and protein concentration. TBARS—thiobarbituric acid-reactive substances; SOD—superoxide dismutase; THB—1,2,3-trihydroxybenzene; abs—absorbance; SH—protein sulfhydryl groups; PER—peroxidases; ORAC—oxygen radical absorbance capacity; NRP—nitrocellulose redox permanganometry; GSH—glutathione; CAT—catalase; and ABTS—2,2′-azino-bis(3-ethylbenzothiazoline-6-sulfonic acid).

https://doi.org/10.1021/acschemneuro.3c00495
ACS Chem. Neurosci. 2023, 14, 4013−4025

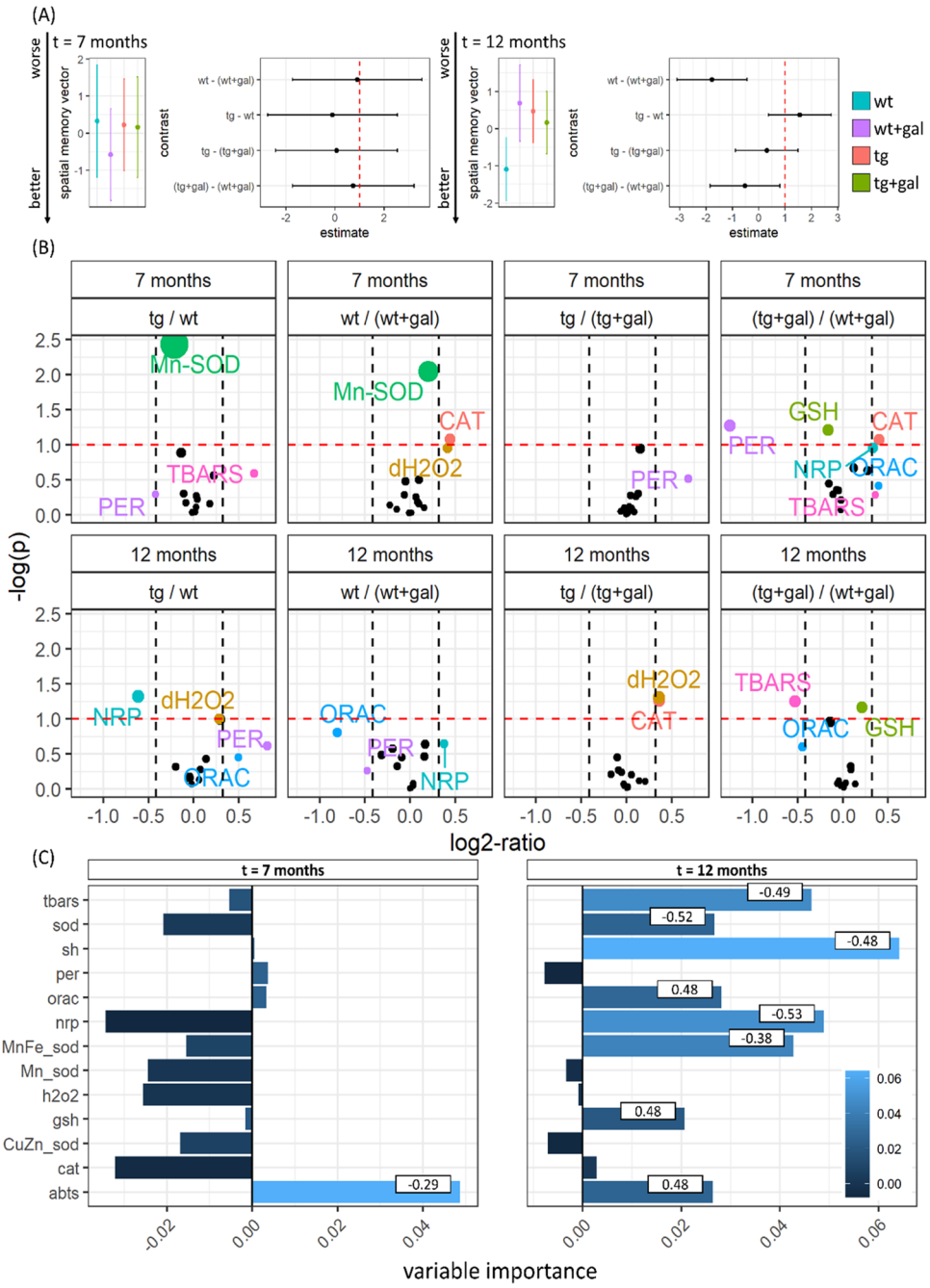

Figure 1. Spatial memory and gastrointestinal redox biomarkers in the presymptomatic (7 months old) and symptomatic (12 months old) Tg2576 mice after chronic oral D-galactose treatment (200 mg/kg). (A) Model output depicting spatial memory vector (SMV) point estimates with 95% confidence intervals (CI) in the presymptomatic (left) and symptomatic (right) Tg2576 mice and respective wild-type controls treated with the vehicle (wt; tg) or oral D-galactose (wt + gal; tg + gal). Larger values are associated with worse performance in the Morris water maze spatial memory test. Group differences are presented as contrasts (point estimates and 95% CI of differences between group least-squares means). (B) Volcano plot demonstrating group comparisons (ratiometric contrasts) with $\log_2$ of ratios on the *X*-axis and $-\log_{10}$ of *p*-values on the *Y*-axis. The exploratory threshold for $-\log_{10}(p)$ is presented as a horizontal red dotted line, and thresholds of the effect size (set at 25%) are denoted as vertical black dotted lines. (C) Variable importance maps calculated based on the permutation-induced mean decrease in accuracy derived from conditional inference-based unbiased classification random forests with SMV defined as the response variable. Bars indicate permutation importance for forest models, and numbers indicate correlation coefficients. abts—difference in absorbance of 2,2′-azino-bis(3-ethylbenzothiazoline-6-sulfonic acid); cat—catalase activity; Cu/Zn-sod—the activity of cytoplasmic Cu/Zn-superoxide dismutase; dh2o2—total H_2O_2 dissociation capacity; gsh—glutathione; h2o2—H_2O_2; Mn-sod—Mn-superoxide dismutase; Mn/Fe-sod—Mn- and Fe-superoxide dismutase; nrp—nitrocellulose redox permanganometry (antioxidant capacity biomarker); orac—oxygen radical absorbance capacity; per—residual activity of peroxidases; sh—protein thiol residues; sod—total superoxide dismutase activity; and tbars—thiobarbituric acid-reactive substances.

microorganisms;[22] and (iii) maintenance of gut redox homeostasis and the GI barrier are mutually intertwined physiological processes.[21,23,24] Until now, investigations into gut redox balance have exclusively focused on the presymptomatic APP/PS1 mouse model of familial AD. In this particular model, researchers observed a decline in the overall antioxidant

https://doi.org/10.1021/acschemneuro.3c00495
ACS Chem. Neurosci. 2023, 14, 4013−4025

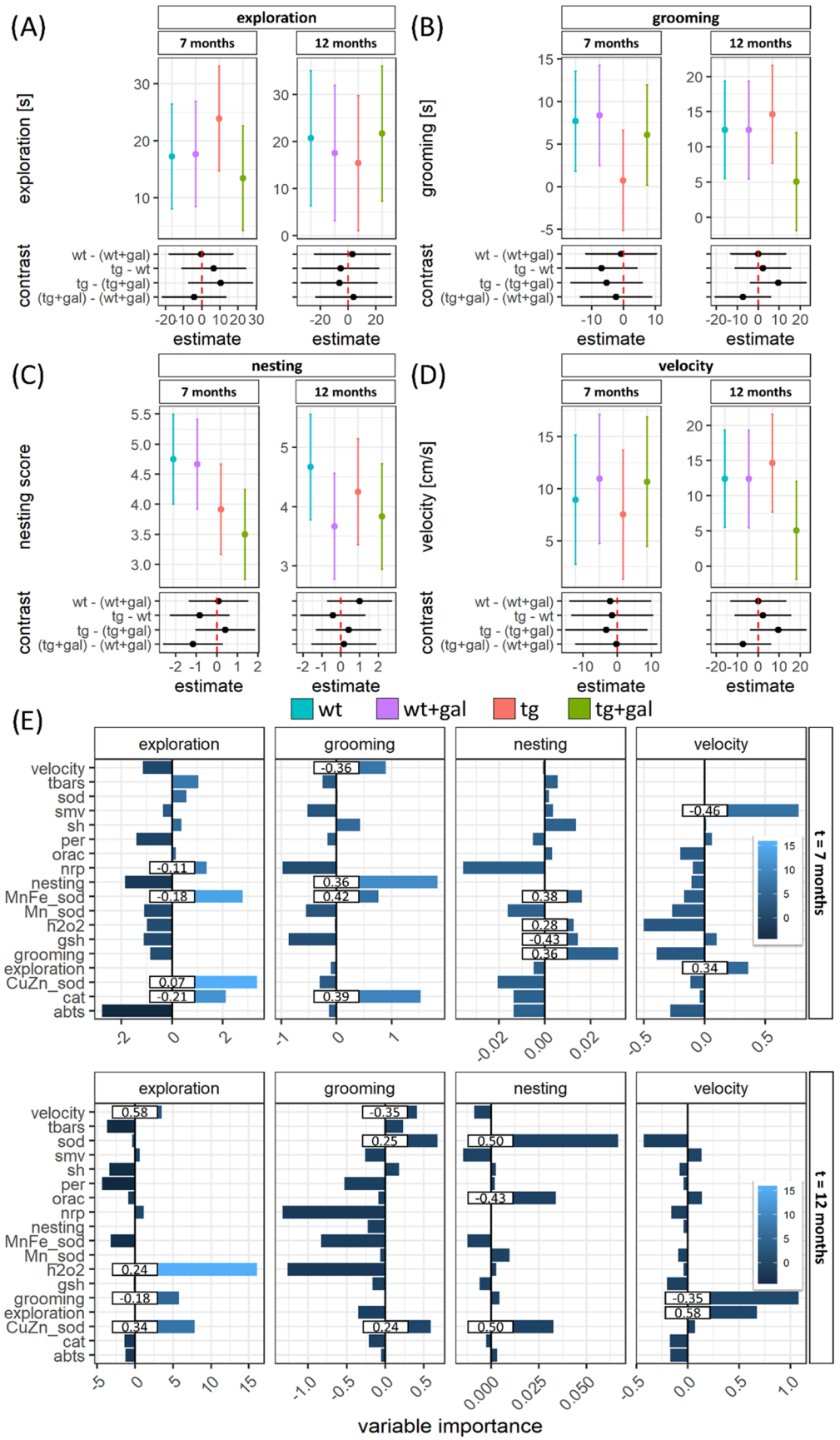

Figure 2. Behavioral characteristics of the presymptomatic (7 months old) and symptomatic (12 months old) Tg2576 mice after chronic oral D-galactose treatment (200 mg/kg). Model output depicting exploratory activity (A), grooming (B), nesting (C), and velocity (D) point estimates and 95% confidence intervals (CI) in the presymptomatic (left) and symptomatic (right) Tg2576 mice and respective wild-type controls treated with the vehicle (wt; tg) or oral D-galactose (wt + gal; tg + gal). Group differences are presented as contrasts (point estimates and 95% CI of

https://doi.org/10.1021/acschemneuro.3c00495
ACS Chem. Neurosci. 2023, 14, 4013−4025

Figure 2. continued

differences between group least-squares means). (E) Variable importance maps calculated based on the permutation-induced mean decrease in accuracy derived from conditional inference-based unbiased classification random forests with exploration, grooming, nesting, and velocity defined as response variables. Bars indicate permutation importance for cforest models and numbers indicate correlation coefficients. abts—difference in absorbance of 2,2′-azino-bis(3-ethylbenzothiazoline-6-sulfonic acid); cat—catalase activity; Cu/Zn-sod—the activity of cytoplasmic Cu/Zn-superoxide dismutase; dh2o2—total H2O2 dissociation capacity; gsh—glutathione; h2o2—H2O2; Mn-sod—Mn-superoxide dismutase; Mn/Fe-sod—Mn- and Fe-superoxide dismutase; nrp—nitrocellulose redox permanganometry (antioxidant capacity biomarker); orac—oxygen radical absorbance capacity; per—residual activity of peroxidases; sh—protein thiol residues; sod—total superoxide dismutase activity; and tbars—thiobarbituric acid-reactive substances.

capacity and a decrease in the expression of genes responsible for preserving and utilizing glutathione (GSH), including GSH S-transferase pi and GSH synthetase.[3] Here, we aimed to examine redox homeostasis in the GI tract of the presymptomatic and symptomatic Tg2576 mice, one of the most widely used transgenic models of AD. Our second aim was to assess the effects of chronic oral D-galactose treatment in the presymptomatic and symptomatic Tg2576 mice and their age-matched controls. Chronic oral D-galactose treatment initiated in the early postinduction period has the potential to prevent and alleviate cognitive dysfunction in the rat model of sporadic AD,[25,26] and recent evidence indicates that oral D-galactose can modulate redox homeostasis in the brain[27] and exert favorable effects on redox signaling in the gut.[28] Finally, considering the importance of the gut−brain axis in regulating behavior,[29−31] we aimed to examine the phenotypic correlates of GI redox biomarkers using data from a behavioral assessment conducted in the same cohort of Tg2576 mice by Babic Perhoc et al.[32]

RESULTS

Presymptomatic Tg2576 had increased activity of gut manganese superoxide dismutase (Mn-SOD; −14% in δTHB absorbance (inversely proportional to Mn-SOD activity); p = 0.004). Increased activity of Mn-SOD was associated with increased lipid peroxidation (+59%), which did not reach the predetermined statistical significance threshold due to large variability. Chronic oral D-galactose treatment (200 mg/kg; ad libitum) was not associated with pronounced changes in gastrointestinal redox biomarkers. The total antioxidant capacity was unaltered. In the wild-type controls, chronic oral D-galactose treatment was associated with decreased H_2O_2 dissociation capacity (−25%) and increased baseline H_2O_2 (+26%), possibly due to the suppressed activity of catalase (−26%; p = 0.08). D-Galactose treatment also increased the activity of superoxide dismutases (SODs), namely, the mitochondrial Mn-SOD (−13% change in 1,2,3-trihydroxybenzene (δTHB) absorbance) (Table 1 and Figure 1) and increased lipid peroxidation (+17%). Interestingly, the observed effect was largely absent in the presymptomatic Tg2576. There was no change in the total H_2O_2 dissociation capacity, the activity of catalase and SOD, or the concentration of lipid peroxidation end products (Table 1 and Figure 1).

In the symptomatic (12 months old) Tg2576, total antioxidant capacity was reduced (nitrocellulose redox permanganometry (NRP): −35%; oxygen radical absorbance capacity (ORAC): +41% (inversely related to antioxidant capacity)) (Table 1 and Figure 1). Total H_2O_2 dissociation capacity (+21%) and the activity of catalase (+23%) and peroxidases were increased, and there was a slight decrease in the Mn-SOD capacity (+10% δTHB absorbance). However, the observed changes were associated with a decreased accumulation of lipid peroxidation end products in the transgenic gastrointestinal tract (−13%) (Table 1 and Figure 1). D-Galactose treatment increased antioxidant capacity (NRP: +12%; ORAC: −9%) and decreased H_2O_2 dissociation capacity only in Tg2576 (−22%), possibly due to suppression of catalase activity (−22%). The observed change in H_2O_2 metabolism following D-galactose in the symptomatic Tg2576 was associated with a slight decrease in GSH availability (+8%). Conversely, D-galactose treatment decreased antioxidant capacity in the gastrointestinal tract of wild-type animals (NRP: −23%; ORAC: +75%). Diminished antioxidant capacity was associated with increased activity of total (−12% δTHB absorbance) and cytoplasmic Cu/Zn-SOD (−11% δTHB absorbance) and decreased activity of mitochondrial Mn-SOD (+15% δTHB absorbance). The observed changes were accompanied by a +24% increased accumulation of lipid peroxidation end products in wild-type animals receiving D-galactose (Table 1 and Figure 1).

Of the observed changes, only gut antioxidant capacity (2,2′-azino-bis(3-ethylbenzothiazoline-6-sulfonic acid) (ABTS) assay) was an important predictor of cognitive performance in the presymptomatic stage (Figure 1C). Mice with a greater gut antioxidant capacity had better cognitive performance (Figure 1C). In the advanced stage, gastrointestinal antioxidant capacity (ABTS, NRP, and ORAC), SOD capacity (total and Mn/Fe-SOD), low-molecular weight and protein thiols, and lipid peroxidation end products were determined to be important predictors of spatial memory (Figure 1C). Greater antioxidant capacity was associated with better cognitive performance based on NRP (r = −0.53) and ORAC (r = 0.48), while ABTS assay (r = 0.48) suggested an inverse association. Both total SOD (δTHB; r = −0.52) and Mn/Fe-SOD (δTHB; r = −0.38) activity were associated with poor cognitive performance, while mitochondrial (Mn-SOD) and cytoplasmic (Cu/Zn-SOD) fractions did not predict spatial memory (Figure 1C). Interestingly, low-molecular weight and protein thiols were both important predictors of cognitive performance; however, low-molecular weight thiols were associated with poor spatial memory, while the inverse was true for protein thiol residues. Cognitive impairment was inversely proportional to the concentration of lipid peroxidation end products in the gastrointestinal tract.

Presymptomatic Tg2576 demonstrated an increased exploration drive and decreased grooming and nesting (Figure 2). D-Galactose treatment normalized exploration and grooming but did not increase the nesting score in the AD model. Conversely, there was no effect of D-galactose on the measured behavioral parameters in the controls. Interestingly, there were no pronounced differences in exploration, grooming, or nesting in the cognitively deficient 12 months old Tg2576, suggesting that the observed phenotypic traits are specific to the presymptomatic phase. D-Galactose treatment was associated

https://doi.org/10.1021/acschemneuro.3c00495
ACS Chem. Neurosci. 2023, 14, 4013−4025

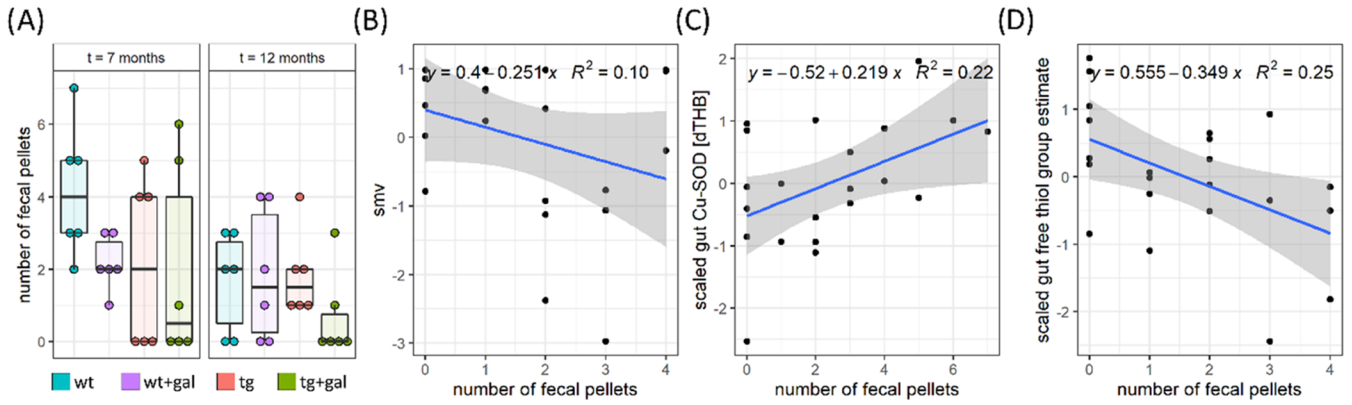

Figure 3. Fecal output is partially associated with redox parameters in the gut but not with smv. Fecal output (A) and the association between fecal output and smv (B), scaled gut Cu-SOD (C), and protein sulfhydryls (D). smv—spatial memory vector and Cu-SOD—Cu/Zn superoxide dismutase.

with reduced grooming behavior and velocity in the open field (OF) test, however, only in 12 months old Tg2576 (Figure 2).

Mn/Fe-SOD was an important predictor of several phenotypic traits in presymptomatic animals (Figure 2E). Greater Mn/Fe-SOD activity was associated with exploration (δTHB; $r = -0.18$) and reduced grooming (δTHB; $r = 0.42$) and nesting (δTHB; $r = 0.38$) scores. The increased exploratory drive was also associated with decreased gut antioxidant capacity (NRP) and decreased gastrointestinal catalase activity ($r = -0.21$). Catalase activity was an important predictor of grooming ($r = 0.39$), while nesting was associated with decreased low-molecular weight thiols ($r = -0.43$) and increased concentration of H_2O_2 ($r = 0.28$) (Figure 2E).

In the symptomatic stage, increased H_2O_2 ($r = 0.24$) and decreased Cu/Zn-SOD activity (δTHB; $r = 0.34$) predicted the exploratory drive. Total and cytoplasmic SOD activity was inversely associated with both grooming (δTHB; total: $r = 0.25$; Cu/Zn-SOD: $r = 0.24$) and nesting (δTHB; total: $r = 0.50$; Cu/Zn-SOD: $r = 0.50$). Nesting was also associated with greater gut antioxidant capacity (ORAC; $r = -0.43$) (Figure 2E).

It has been hypothesized that redox biomarkers might be associated with GI function and thus possibly reflected in fecal pellet output. Total fecal pellet output was unremarkable both in the 7 months old and 12 months old animals (Figure 3A). In the presymptomatic stage, chronic oral D-galactose treatment was associated with fewer pellets produced in the 7 months old wild-type animals; however, there was no change in the Tg2576. There was no association between fecal pellet output and spatial memory in the 7 months old mice (spatial memory vector (smv) vs fecal pellet output; $r = 0.03$); however, 12 months old mice with poor spatial memory produced fewer pellets on average (smv vs fecal pellet output; $r = -0.32$) (Figure 3B). Redox biomarkers demonstrated variable associations with the fecal pellet output. The strongest association was observed for cytoplasmic SOD in the 7 months old mice (Figure 3C) and protein thiol groups in the 12 months old animals (Figure 3D). In both cases, a greater antioxidant capacity was associated with the production of fewer pellets. Associations between fecal pellet output and all redox biomarkers are provided in the Supporting information.

Finally, we analyzed the association between GI redox biomarkers measured in this study and the expression of plasma and brain metabolic and neuropathological markers measured by Babic Perhoc et al. in the same cohort of Tg2576 mice.[32] Correlations between all parameters are provided in the Supporting information.

DISCUSSION

The presented results suggest an increased electrophilic burden in the Tg2576 gut compensated for by the time the animals develop cognitive deficits. Chronic oral D-galactose administration is associated with detrimental effects in the gut of wild-type animals but not in the Tg2576 GI tract, providing evidence in favor of the hypothesis that the beneficial effects of D-galactose might depend on the underlying pathophysiology. Gut redox biomarkers seem to be associated with behavioral patterns across groups with the most pronounced contribution related to spatial memory in the advanced stage of the disease possibly reflecting the behavioral effects mediated by the gut−brain axis.[33]

Although the effects were small and accompanied by large uncertainty (due to the exploratory nature of the experiment), redox biomarkers suggest that an increased GI electrophilic burden might precede the development of cognitive deficits in Tg2576. The activity of the mitochondrial antioxidant enzyme Mn-SOD was increased in the gut of presymptomatic Tg2576, possibly indicating a compensatory response to increased generation of $O_2^{\bullet-}$ anions (Table 1, Figures 1 and 2). Increased expression and activity of Mn-SOD represent important mechanisms by which cells defend against the accumulation of free radicals generated in the process of mitochondrial respiration.[34,35] The activity of cytoplasmic Cu/Zn-SOD and bacterial Fe-SOD did not change, indicating that the electrophilic burden in the Tg2576 gut might be primarily related to mitochondrial metabolism. The hypothesis that increased Mn-SOD represents a compensatory response is supported by the finding of increased accumulation of thiobarbituric acid-reactive substances (TBARS), indicating either failure of upstream antioxidant defense systems in preventing initiation of lipid peroxidation or the inability of terminating mechanisms to stop its propagation.[36] In the symptomatic Tg2576, Mn-SOD activity was decreased, possibly as a result of prolonged exposure to increased concentration of free radicals.[37] Moreover, total antioxidant capacity was decreased, and the activities of H_2O_2-metabolizing systems (catalase and peroxidases) were increased (Table 1, Figures 1 and 2). Increased wasting of nucleophilic substrates (reflected in reduced antioxidant capacity) and upregulation of H_2O_2 metabolism were accompanied by

https://doi.org/10.1021/acschemneuro.3c00495
ACS Chem. Neurosci. 2023, 14, 4013−4025

neutralization of lipid peroxidation, suggesting that compensatory mechanisms were able to stabilize increased generation of free radicals by redefining a redox heterostatic set point most likely at the expense of long-term functioning.[18,38] The observed results, suggesting an increased electrophilic burden in the presymptomatic stage heterostatically compensated by the time the animals developed cognitive deficits, are in line with previous reports in other animal models of familial AD. Chi et al. reported reduced expression of enzymes involved in GSH-mediated defense against oxidative stress and decreased total antioxidant capacity in the GI tract of the presymptomatic APP/PS1 mice.[3] Honarpisheh et al. did not assess GI redox homeostasis; however, they observed multiple pathophysiological alterations in presymptomatic Tg2576 that did not persist to the symptomatic stage.[4] Early pathophysiological alterations observed by Honarpisheh et al. in the presymptomatic Tg2576 might be associated with unopposed electrophilic burden, while the establishment of redox heterostasis corresponds with the absence of structural and functional changes of the GI barrier in the aged mice.[4] The precise factors contributing to the unexpected electrophilic stress observed in presymptomatic Tg2576 mice have yet to be fully understood. However, it is important to highlight that an imbalance in gut microbiota, as evidenced in the Tg2576 model,[39] may have a role in perturbing the host's intestinal redox equilibrium. A disrupted gut microbial environment could potentially contribute to the production of free radicals through various mechanisms such as disturbing the integrity of the intestinal barrier, inciting inflammation, or even directly influencing intestinal mitochondria. This influence on intestinal mitochondria could trigger mitochondrial dysfunction-associated senescence (MiDAS) through a bidirectional communication, given the shared evolutionary ancestry of mitochondria and bacteria.[14]

The dysfunction of intestinal mitochondria and the compromised function of the gastrointestinal barrier subsequently lead to inflammation and an increased generation of detrimental free radicals, ultimately impacting the delicate balance of both the central nervous system and overall systemic health.[19,21]

Chronic oral D-galactose treatment was associated with detrimental effects on redox homeostasis in the 7 and 12 months old wild-type mice; however, in the Tg2576, the effects of D-galactose were either absent (presymptomatic stage) or associated with beneficial modulation of redox homeostasis (symptomatic stage). Chronic parenteral administration of D-galactose is widely utilized for the induction of oxidative stress and modeling aging,[40,41] so its detrimental effects on redox homeostasis in wild-type animals are not surprising. Nevertheless, harmful effects of chronic D-galactose treatment are usually observed after parenteral administration of large doses, while chronic oral ad libitum administration has so far only been associated with beneficial effects in animal models of AD[25,26,32] and atopic dermatitis.[42] A large body of evidence suggests that the majority of the harmful and beneficial effects of D-galactose might be explained by tissue exposure. Peroral administration of D-galactose, associated with beneficial effects, usually results in 10-fold lower tissue exposure in comparison with parenteral routes due to intestinal absorption and liver retention.[27,28,43,44] In contrast, bolus oral administration can exceed tissue buffering capacity and achieve high plasma D-galactose concentrations[25] and has, thus, been associated with detrimental effects.[45,46] Likewise, parenteral (i.e., subcutaneous) administration of D-galactose can exert beneficial effects[47] if tissue metabolic capacity is not exceeded. Nevertheless, there are some exceptions (e.g., a recent report of beneficial effects of large-dose parenteral D-galactose in irradiated mice[48]) and it cannot be excluded that the effects of D-galactose are not only dose- but also model-dependent.[43,49] The presented results support this concept, as detrimental effects of chronic oral D-galactose on gut redox homeostasis (and cognition) were observed only in the wild-type controls.

One of our aims was to explore whether GI redox biomarkers are valid predictors of mouse behavior. Recent evidence strongly supports the role of gut microbiota in regulating animal behavior;[29−31] however, exact mechanisms used by gut microbiota to control behavioral patterns are still not fully understood. Considering a close relationship between gut eubiosis and GI redox homeostasis,[50−54] the gut redox milieu might be associated with specific behavioral patterns. In this research, GI antioxidant capacity (ABTS) was recognized as a potential predictor of cognitive performance across groups, with greater antioxidant capacity associated with better spatial memory in the 7 months old mice. In the 12 months old mice, several biomarkers were recognized as potential predictors of cognitive performance. NRP, ORAC, and concentration of protein thiols and the increased antioxidant capacity predicted better overall spatial memory; however, lipid peroxidation, GSH, and lower activity of total and Mn/Fe-SOD were also paradoxically recognized as positive predictors of cognitive performance. Discrepant results suggest that the relationship between GI redox homeostasis and cognitive performance cannot be described by a simple model in which better redox homeostasis translates to improved spatial memory. The understudied direct and indirect (e.g., blood flow-mediated) effects of meal ingestion on intraluminal redox homeostasis provide one possible explanation for the paradoxical findings. The latter is supported by the recognition of Mn/Fe-SOD as one of the predictors, as this enzyme is found in plants and bacteria. In this context, the reduced activity of Mn/Fe-SOD, associated with better spatial memory, might reflect either suppressed microbiota-derived SOD or the absence of food ingestion shortly before the trial. Unfortunately, temporal patterns of food intake were not monitored in the present study. Mn/Fe-SOD also predicted other behavioral patterns: its activity was associated with exploration and inversely associated with grooming and nesting scores in the 7 months old cohort. Nesting was associated with greater baseline H_2O_2 and reduced GSH, while catalase activity acted as a positive predictor of grooming and a negative predictor of exploration. In the 12 months old mice, total and cytoplasmic SOD activity demonstrated an inverse correlation with grooming and nesting, while the decreased activity of Cu/Zn-SOD and decreased baseline H_2O_2 predicted greater exploration. The latter might reflect inflammatory signaling associated with the generation of $O_2^{\bullet-}$[55] as it has been shown that even mild inflammation is sufficient to induce anxiety-like behavior.[56] More research is needed to understand the biological implications of the observed associations.

Finally, we found no evidence of a strong association between the fecal pellet output and spatial memory. In the presymptomatic stage, there was no association, while in the symptomatic stage, there was only a weak association between cognitive ability and the number of fecal pellets. The number of fecal pellets was associated with some redox biomarkers, possibly indicating the reduced antioxidant capacity in animals

https://doi.org/10.1021/acschemneuro.3c00495
ACS Chem. Neurosci. 2023, 14, 4013−4025

producing more pellets; however, the relationship between redox homeostasis and GI function remains to be elucidated.

CONCLUSIONS

The presented results indicate an electrophilic challenge of the GI redox homeostasis in Tg2576 mice before the development of cognitive deficits compensated by the time the animals develop symptoms. The results suggest that gut oxidative stress might be involved in the processes driving the initiation of neurodegenerative changes. Alternatively, subtle CNS changes taking place in the early stage of neurodegeneration might affect gut redox homeostasis, while the animals are still not manifesting cognitive deficits. Future research should elucidate whether the observed changes might contribute to neurodegenerative processes by supporting peripheral inflammation.

LIMITATIONS

The most important limitation of this study is its exploratory design with only 5−6 animals per group. Consequently, the power to detect changes in some redox biomarkers with satisfactory certainty was fairly low. For example, in the presymptomatic Tg2576, lipid peroxidation in the gut was increased by ∼60%, indicating a relatively large and likely biologically meaningful effect. Nevertheless, the effect did not meet the predetermined criteria for statistical significance due to a small number of animals and relatively large dispersion. We fixed α at 10% to minimize the risk of omission and avoid an excessive false nondiscovery rate; however, evident from the above-mentioned example, it is reasonable to assume that some relevant effects might have still been missed and additional studies are needed to better understand the role of GI redox homeostasis in transgenic models of AD. Another limitation is that temporal patterns of food intake were not monitored in the present study. As it can be speculated that the presence of intraluminal nutrients might exert both direct and indirect effects on redox homeostasis of the gut, it cannot be ruled out that some of the effects reflected the difference in meal timing caused by either genotype or D-galactose treatment.

MATERIALS AND METHODS

Animals. 40 adult male B6;SJL-Tg(APPSWE)2576Kha heterozygous transgenic mice (Tg2576) and wild-type controls aged 5 months and 40 mice aged 10 months (Taconic Biosciences Inc., Hudson New York) entered the experiments. Mice were housed individually in standard cages in vented positive-pressure cabinets maintaining a stable temperature (22−24 °C) and humidity (40−60%) environment, with a 12 h light/12 h dark cycle, at the licensed animal facility at the Croatian Institute for Brain Research, University of Zagreb School of Medicine (HR-POK-006). Mice were kept on standardized food pellets and water ad libitum before galactose treatment was initiated, after which treated groups received galactose dissolved in tap water in the previously observed daily water intake volume with tap water made available after the daily dose was consumed.

Experimental Design. The first mouse cohort of 40 animals entered the experiment at 5 months old, to assess the characteristics of presymptomatic fAD, whereas the second cohort investigating symptomatic fAD started the experiment at 10 months old. In both instances, mice were divided into 4 groups with 10 animals per group: Tg2576 (tg), wild types (wt), galactose-treated Tg2576 (tg + gal), and galactose-treated wild types (wt + gal). Oral D-galactose treatment lasted for 2 months, when the animals underwent cognitive and behavioral testing as indicated below (aged 7 and 12 months, respectively). Following these tests, animals were sacrificed, and samples were withdrawn for further analyses. Tissue samples used in this study were from the same animals used in the study by Babic Perhoc et al. for the assessment of the effects of D-galactose on metabolic parameters in the CNS.[32]

Galactose Treatment. Oral D-galactose treatment lasted for two months and was initiated in the two cohorts at 5 and 10 months of age, respectively. D-Galactose was freshly dissolved in tap water at a concentration of 200 mg/kg/day, in a volume previously observed as the average daily water intake for each animal (∼10 mL daily). Control Tg2576 and wild-type mice received regular tap water throughout the experiment.

Behavioral Analysis. Behavioral assessment was based on a battery of tests, including the Morris water maze (MWM), OF, and nesting assessment. Technical details of MWM and OF are described in detail in the original publication.[32] MWM was performed following a previously described protocol.[57] The test was conducted for a total of 6 trial days, which included 5 learning and memory trial days, each with 4 trials per day (each from a different starting point; southwest (SW), south (S), east (E), and northeast (NE), separated by 30 min of rest periods), and a probe trial on day 6. Mice were placed in a 120 cm-diameter round pool filled with water at a temperature of 25 ± 1 °C and 60 cm deep. During the first 5 training days, mice were trained to escape the water by finding a concealed 15 cm-diameter wide, glass platform, which was submerged 2 cm below the water surface and placed in the same quadrant of the pool on each training day (northwestern (NW) quadrant). Mice which successfully found the platform during the 60 s long trial remained on it for 15 s to memorize its location. Mice that completed the trial without finding the platform were lured toward it to allow the animals to learn its location. Escape latency was recorded, defined as the time needed to find the platform after being released from the pool. The probe trial which assessed the mice's memory retention was performed on the sixth day by releasing the mice from the southeastern (SE) quadrant and with the platform removed from the pool. Memory retention was reflected in the time spent in the search for the platform in the correct quadrant. Data were acquired using a Basler AG camera and tracked and analyzed using EthoVision XT software (Noldus Information Technology). Spatial memory parameters from the original study[32] were dedimenzionalized into a single spatial memory vector parameter (described in the Data Analysis section).

OF was performed in a square chamber (50 cm × 50 cm × 40 cm) positioned in a normally lit room. Animals were placed in the arena and observed for 5 min, with their movement recorded using a camera (Basler AG) and tracked and analyzed using video software (EthoVision XT, Noldus Information Technology). Each animal was placed in the same corner of the previously wiped chamber and left to explore for 5 min. Grooming, velocity, and exploration drive were assessed by using EthoVisionXT software.

Nesting was performed according to a predefined protocol[58] before sacrification. Individually housed mice were given a small rectangle (approximately 5 cm × 5 cm) of pressed cotton an hour before the dark cycle. On the following morning, each cage was assessed by two observers and given a score on a rating scale of 1−5, as indicated,[58] with 1 representing the lowest score and more than 90% of the piece of cotton left untouched and 5 representing a near-perfect nest. The average score from both investigators was recorded for each built nest.

Fecal Pellet Output. Fecal pellet output was measured by counting the number of fecal pellets produced in the OF arena over 300 s.

Sample Preparation. The animals were euthanized by decapitation in deep anesthesia (thiopental 60 mg/kg/diazepam 6 mg/kg ip). Internal organs were exposed by laparotomy, and the duodenum was removed and snap-frozen in liquid nitrogen and stored at −80 °C. Frozen tissue sections were thawed in lysis buffer (150 mM NaCl, 50 mM Tris-HCl pH 7.4, 1 mM EDTA, 1% Triton X-100, 1% sodium deoxycholate, 0.1% SDS, 1 mM PMSF, protease (Sigma-Aldrich, Burlington, Massachusetts) and phosphatase (PhosSTOP, Roche, Basel, Switzerland) inhibitor cocktail; pH 7.5) and subjected to three cycles of ultrasonic homogenization (Microson Ultrasonic Cell 167 Disruptor XL, Misonix, Farmingdale, NY, SAD). Homogenates were

https://doi.org/10.1021/acschemneuro.3c00495
ACS Chem. Neurosci. 2023, 14, 4013−4025

centrifuged for 10 min (relative centrifugal force 12 879 g), and protein concentration was measured using the Bradford reagent (Sigma-Aldrich). A protein calibration curve was determined with bovine serum albumin dissolved in lysis buffer. Homogenates were kept at −80 °C.

Antioxidant Capacity. Antioxidant capacity was determined with three separate biochemical methods. The ABTS radical cation assay was performed by measuring the change in absorbance of the ABTS working solution after incubation in the presence of tissue samples in a 96-microwell plate. ABTS (7 mM) was incubated with $K_2S_2O_8$ (2.45 mM) for 24 h. ABTS/$K_2S_2O_8$ solution was diluted 40-fold and incubated with 1 μL of each homogenate in a volumetric ratio of 1:100 (sample/ABTS). The absorbance at 405 nm was measured after 5 min using an Infinite F200 PRO multimodal microplate reader (Tecan, Switzerland).[10] The difference between the baseline control solution (ABTS) and final absorbance was proportional to the sample antioxidant capacity.[59] The ORAC fluorescein assay was conducted by incubating tissue samples (10 μL) with 150 μL of 5 μM fluorescein dissolved in phosphate-buffered saline (pH 7) in a 96-microwell plate.[60] Fluorescence (465 nm excitation/540 nm emission; 10 nm bandwidth) was recorded every minute for 60 min using an Infinite F200 PRO multimodal microplate reader (Tecan, Switzerland). NRP was performed by quantifying the sample-mediated reduction of $KMnO_4$ by measuring the integrated density of the MnO_2 precipitate on a nitrocellulose membrane. Briefly, 1 μL of each sample was pipetted onto the nitrocellulose membrane (Amersham Protran 0.45; GE Healthcare Life Sciences, Chicago, Illinois), and the dry membrane was incubated in NRP solution (0.01 g/mL of $KMnO_4$ in ddH_2O) for 30 s. The membrane was destained in ddH_2O, digitalized, and analyzed in Fiji with the gel analyzer plugin.[61]

Catalase/Peroxidase Activity and H_2O_2 Concentration. The activity of catalase and peroxidases and baseline concentration of H_2O_2 were measured by the assay originally proposed by Hadwan[62] and adapted and validated in our previous publications.[63−65] Briefly, tissue samples (5 μL) were incubated with 150 μL of $Co(NO_3)_2$ solution (0.1 g of $Co(NO_3)_2 \times 6\ H_2O$ in 5 mL of ddH_2O mixed with $(NaPO_3)_6$ solution (0.05 g of $(NaPO_3)_6$ dissolved in 5 mL of ddH_2O) and added to 90 mL of $NaHCO_3$ solution (8.1 g in 90 mL ddH_2O)) in a microwell plate to obtain baseline H_2O_2 concentrations. The same procedure was repeated after incubating the samples with 10 mM H_2O_2 in PBS for 90 s to measure total H_2O_2 dissociation capacity and in the presence of 10 mM H_2O_2 and 0.025 mM NaN_3 in PBS to measure the NaN_3-insensitive fraction reflecting the activity of peroxidases.[64,66] The H_2O_2 concentration was estimated from the ($[Co(CO_3)_3]Co$) absorbance at 450 nm using an Infinite F200 PRO multimodal microplate reader (Tecan, Switzerland) based on the linear model obtained with serial dilutions of H_2O_2 in PBS (R^2 = 0.97−0.99). Assay sensitivity was optimized by modifying sample volumes and reaction times based on pilot experiments on the same samples.

SOD Activity. The activity of SOD was analyzed utilizing an indirect assay based on the inhibition of THB autoxidation introduced by Marklund and Marklund[67] and modified by others.[28,68] Briefly, tissue samples (6 μL) were incubated with 100 μL of the SOD working solution, THB solution (80 μL; 60 mM THB in 1 mM HCl), mixed with 4000 μL of the reaction buffer (0.05 M Tris-HCl and 1 mM Na_2EDTA in ddH_2O; pH 8.2) in a 96-well plate for 300 s. The absorbance increase at 450 nm reflecting THB autoxidation was measured with kinetic intervals of 30 s to approximate SOD activity. The same procedure was repeated with modified reaction buffers containing inhibitors partially selective for Cu/Zn-SOD (2 mM KCN) or Cu/Zn-SOD and Fe-SOD (5 mM H_2O_2).[64,66]

Protein and Low-Molecular Weight Thiol Group Quantification. Free thiol groups were quantified with Ellman's procedure based on the reaction of sulfhydryl residues with 5,5′-dithio-bis(2-nitrobenzoic acid)(DTNB), which yields a yellow-colored product, 5-thio-2-nitrobenzoic acid (TNB).[9,27,69] Tissue homogenates (25 μL) were mixed with an equal amount of 4% sulfosalicylic acid solution for 60 min on ice, and the samples were centrifuged for 10 min at 10 000*g* to obtain the protein (pellet) and low-molecular weight (supernatant) fractions. Both fractions were incubated with the DTNB solution (4 mg/mL DTNB in 5% sodium citrate) at room temperature for 10 min, and 405 nm absorbance was measured with an Infinite F200 PRO multimodal microplate reader (Tecan, Switzerland). The concentration of thiol residues was estimated based on the extinction coefficient of 14 150 $M^{-1}cm^{-1}$.

Lipid Peroxidation. Lipid peroxidation was measured with the modified TBARS assay[70] as described previously.[27,28] Briefly, tissue homogenates (12 μL) were incubated with 120 μL of the TBA-TCA reagent (0.4% thiobarbituric acid in 15% trichloroacetic acid) in a heating block set at 95 °C for 20 min in perforated microcentrifuge tubes. The colored adduct was extracted with *n*-butanol (100 μL), and the absorbance was measured at 540 nm using the Infinite F200 PRO multimodal microplate reader (Tecan, Switzerland). The concentration of TBARS was determined from the linear model obtained with serial dilutions of malondialdehyde (Sigma-Aldrich) (R^2 = 0.98−0.99). The procedure was optimized for the analysis of duodenal homogenates by iterative adjustment of the sample volume, reaction time, and the *n*-butanol extraction procedure.

Data Analysis. Data were analyzed using R (4.1.3) following ARRIVE 2.0 guidelines for reporting animal studies.[71] Gastrointestinal redox biomarkers were analyzed by fitting linear models using the biomarker of interest as the dependent variable, while group allocation (based on the treatment and genotype) and protein concentration (loading control) were defined as independent predictors. Additional covariates were introduced where necessary: baseline concentration of H_2O_2 (total H_2O_2 dissociation capacity, catalase, and peroxidase activity models); peroxidase activity (catalase activity model); and Mn/Fe-SOD activity (Cu/Zn-SOD activity model). The effect of age was not modeled directly as it was not permitted by the experimental design (separate cohorts). A change in THB absorbance (inversely proportional to SOD activity) was used in modeling instead of approximated activity measures of SOD to reduce artifactual uncertainty. Visual inspection of residuals was performed to check model assumptions, and appropriate (log) transformations were introduced where appropriate. Model outputs (group least-squares means and their contrasts) were reported as point estimates with 95% confidence intervals (CI). Contrasts were reported as ratios regardless of the presence of log transformation in the original model to facilitate the interpretation of effect sizes. Considering the exploratory nature of the study, α was set at 10% to deflate the type II error and avoid excessive false nondiscovery rate (particularly for large effects) (e.g., the threshold for $-\log_{10}(p)$ was fixed at 1 in the volcano plot).[72] Complex variables (e.g., MWM indices of spatial memory) were dedimensionalized with principal component analysis (conducted on a centered, scaled, and mean-imputed data set) to obtain a single biologically meaningful variable (e.g., spatial memory vector (smv)). Smv for the presymptomatic and symptomatic stages captured 66.2 and 94.7% of the variance (quadrant preference in training and test trials), respectively. Correlation matrices were based on the Pearson and Spearman correlation coefficients. Variable importance was determined using the permutation-induced mean decrease in accuracy derived from conditional inference-based unbiased classification random forests in the computational toolbox for recursive partitioning (party).[73]

■ ASSOCIATED CONTENT

Data Availability Statement

Raw data can be obtained from the corresponding author. The article has been preprinted on bioRxiv (10.1101/2023.06.03.542513).

Supporting Information

The Supporting Information is available free of charge at https://pubs.acs.org/doi/10.1021/acschemneuro.3c00495.

Analysis of correlations between functional and behavioral outcomes, redox biomarkers, and molecules associated with metabolic signaling pathways in the gut and the brains of mice aged 7 and 12 months (PDF)

https://doi.org/10.1021/acschemneuro.3c00495
ACS Chem. Neurosci. 2023, 14, 4013−4025

AUTHOR INFORMATION

Corresponding Author

Jan Homolak − *Department of Pharmacology, University of Zagreb School of Medicine, Zagreb 10000, Croatia; Croatian Institute for Brain Research, University of Zagreb School of Medicine, Zagreb 10000, Croatia; Interfaculty Institute of Microbiology and Infection Medicine, University of Tübingen, Tübingen 72076, Germany; Cluster of Excellence "Controlling Microbes to Fight Infections", University of Tübingen, Tübingen 72076, Germany;* orcid.org/0000-0003-1508-3243; Email: homolakjan@gmail.com, jan.homolak@mef.hr

Authors

Ana Babic Perhoc − *Department of Pharmacology, University of Zagreb School of Medicine, Zagreb 10000, Croatia; Croatian Institute for Brain Research, University of Zagreb School of Medicine, Zagreb 10000, Croatia*

Ana Knezovic − *Department of Pharmacology, University of Zagreb School of Medicine, Zagreb 10000, Croatia; Croatian Institute for Brain Research, University of Zagreb School of Medicine, Zagreb 10000, Croatia*

Jelena Osmanovic Barilar − *Department of Pharmacology, University of Zagreb School of Medicine, Zagreb 10000, Croatia; Croatian Institute for Brain Research, University of Zagreb School of Medicine, Zagreb 10000, Croatia*

Davor Virag − *Department of Pharmacology, University of Zagreb School of Medicine, Zagreb 10000, Croatia; Croatian Institute for Brain Research, University of Zagreb School of Medicine, Zagreb 10000, Croatia*

Melita Salkovic-Petrisic − *Department of Pharmacology, University of Zagreb School of Medicine, Zagreb 10000, Croatia; Croatian Institute for Brain Research, University of Zagreb School of Medicine, Zagreb 10000, Croatia*

Complete contact information is available at: https://pubs.acs.org/10.1021/acschemneuro.3c00495

Author Contributions

A.B.P., A.K., and J.O.B.: treatment and behavioral experiments; J.H. and A.B.P.: biochemical analyses, data curation, data analysis, and writing the first draft of the article. A.K., J.O.B., D.V., and M.S.P.: critical revision of the article. M.S.P.: funding and supervision.

Funding

This work was funded by the Croatian Science Foundation (IP-2018-01-8938; IP-2014-09-4639). The research was cofinanced by the Scientific Centre of Excellence for Basic, Clinical, and Translational Neuroscience (project "Experimental and clinical research of hypoxic-ischemic damage in perinatal and adult brain"; GA KK01.1.1.01.0007 funded by the European Union through the European Regional Development Fund).

Notes

The authors declare no competing financial interest.

The animal procedures were conducted in concordance with the current institutional (University of Zagreb School of Medicine), national (The Animal Protection Act, NN135/2006; NN 47/2011), and international (Directive 2010/63/EU) guidelines on the use of experimental animals. The experiments were approved by the Croatian Ministry of Agriculture (EP 186/2018; 525-10/0255-15-5) and the Ethical Committee of the University of Zagreb School of Medicine (380-59-10106-18-111/173).

REFERENCES

(1) Singh, A.; Dawson, T. M.; Kulkarni, S. Neurodegenerative Disorders and Gut-Brain Interactions. *J. Clin. Invest.* **2021**, *131* (13), No. e143775, DOI: 10.1172/JCI143775.

(2) Sun, M.; Ma, K.; Wen, J.; Wang, G.; Zhang, C.; Li, Q.; Bao, X.; Wang, H. A Review of the Brain-Gut-Microbiome Axis and the Potential Role of Microbiota in Alzheimer's Disease. *J. Alzheimer's Dis.* **2020**, *73* (3), 849−865, DOI: 10.3233/JAD-190872.

(3) Chi, H.; Cao, W.; Zhang, M.; Su, D.; Yang, H.; Li, Z.; Li, C.; She, X.; Wang, K.; Gao, X.; Ma, K.; Zheng, P.; Li, X.; Cui, B. Environmental Noise Stress Disturbs Commensal Microbiota Homeostasis and Induces Oxi-Inflammmation and AD-like Neuropathology through Epithelial Barrier Disruption in the EOAD Mouse Model. *J. Neuroinflammation* **2021**, *18* (1), 9.

(4) Honarpisheh, P.; Reynolds, C. R.; Blasco Conesa, M. P.; Moruno Manchon, J. F.; Putluri, N.; Bhattacharjee, M. B.; Urayama, A.; McCullough, L. D.; Ganesh, B. P. Dysregulated Gut Homeostasis Observed Prior to the Accumulation of the Brain Amyloid-β in Tg2576 Mice. *Int. J. Mol. Sci.* **2020**, *21* (5), 1711.

(5) Manocha, G. D.; Floden, A. M.; Miller, N. M.; Smith, A. J.; Nagamoto-Combs, K.; Saito, T.; Saido, T. C.; Combs, C. K. Temporal Progression of Alzheimer's Disease in Brains and Intestines of Transgenic Mice. *Neurobiol. Aging* **2019**, *81*, 166−176.

(6) Semar, S.; Klotz, M.; Letiembre, M.; Van Ginneken, C.; Braun, A.; Jost, V.; Bischof, M.; Lammers, W. J.; Liu, Y.; Fassbender, K.; Wyss-Coray, T.; Kirchhoff, F.; Schäfer, K.-H. Changes of the Enteric Nervous System in Amyloid-β Protein Precursor Transgenic Mice Correlate with Disease Progression. *J. Alzheimer's Dis.* **2013**, *36* (1), 7−20, DOI: 10.3233/JAD-120511.

(7) Wang, Y.; An, Y.; Ma, W.; Yu, H.; Lu, Y.; Zhang, X.; Wang, Y.; Liu, W.; Wang, T.; Xiao, R. 27-Hydroxycholesterol Contributes to Cognitive Deficits in APP/PS1 Transgenic Mice through Microbiota Dysbiosis and Intestinal Barrier Dysfunction. *J. Neuroinflammation* **2020**, *17* (1), 199.

(8) Homolak, J.; Babic Perhoc, A.; Knezovic, A.; Osmanovic Barilar, J.; Koc, F.; Stanton, C.; Ross, R. P.; Salkovic-Petrisic, M. Disbalance of the Duodenal Epithelial Cell Turnover and Apoptosis Accompanies Insensitivity of Intestinal Redox Homeostasis to Inhibition of the Brain Glucose-Dependent Insulinotropic Polypeptide Receptors in a Rat Model of Sporadic Alzheimer's Disease. *Neuroendocrinology* **2022**, *112* (8), 744−762.

(9) Homolak, J.; Babic Perhoc, A.; Knezovic, A.; Osmanovic Barilar, J.; Salkovic-Petrisic, M. Failure of the Brain Glucagon-Like Peptide-1-Mediated Control of Intestinal Redox Homeostasis in a Rat Model of Sporadic Alzheimer's Disease. *Antioxidants* **2021**, *10* (7), 1118.

(10) Homolak, J.; De Busscher, J.; Zambrano-Lucio, M.; Joja, M.; Virag, D.; Babic Perhoc, A.; Knezovic, A.; Osmanovic Barilar, J.; Salkovic-Petrisic, M. Altered Secretion, Constitution, and Functional Properties of the Gastrointestinal Mucus in a Rat Model of Sporadic Alzheimer's Disease. *ACS Chem. Neurosci.* **2023**, *14*, 2667−2682, DOI: 10.1021/acschemneuro.3c00223.

(11) Qian, X.-H.; Liu, X.-L.; Chen, G.; Chen, S.; Tang, H.-D. Injection of Amyloid-β to Lateral Ventricle Induces Gut Microbiota Dysbiosis in Association with Inhibition of Cholinergic Anti-Inflammatory Pathways in Alzheimer's Disease. *J. Neuroinflammation* **2022**, *19* (1), 236.

(12) Alves, S. S.; Silva-Junior, R. M.; Servilha-Menezes, G.; Homolak, J.; Šalković-Petrišić, M.; Garcia-Cairasco, N. Insulin Resistance as a Common Link Between Current Alzheimer's Disease Hypotheses. *J. Alzheimer's Dis.* **2021**, *82* (1), 71−105, DOI: 10.3233/JAD-210234.

(13) Brown, G. C. The Endotoxin Hypothesis of Neurodegeneration. *J. Neuroinflammation* **2019**, *16* (1), 180 DOI: 10.1186/s12974-019-1564-7.

(14) Homolak, J. Targeting the Microbiota-Mitochondria Crosstalk in Neurodegeneration with Senotherapeutics. *Adv. Protein Chem.*

Struct. Biol. **2023**, *136*, 339−383, DOI: 10.1016/bs.apcsb.2023.02.018.
(15) Qian, X.-H.; Song, X.-X.; Liu, X.-L.; Chen, S.; Tang, H.-D. Inflammatory Pathways in Alzheimer's Disease Mediated by Gut Microbiota. *Ageing Res. Rev.* **2021**, *68*, No. 101317, DOI: 10.1016/j.arr.2021.101317.
(16) Soto, M.; Herzog, C.; Pacheco, J. A.; Fujisaka, S.; Bullock, K.; Clish, C. B.; Kahn, C. R. Gut Microbiota Modulate Neurobehavior through Changes in Brain Insulin Sensitivity and Metabolism. *Mol. Psychiatry* **2018**, *23* (12), 2287−2301.
(17) Butterfield, D. A.; Halliwell, B. Oxidative Stress, Dysfunctional Glucose Metabolism and Alzheimer Disease. *Nat. Rev. Neurosci.* **2019**, *20* (3), 148−160.
(18) Homolak, J. Redox Homeostasis in Alzheimer's Disease. In *Redox Signaling and Biomarkers in Ageing*; Çakatay, U., Ed.; Springer International Publishing: Cham, 2022; pp 323−348 DOI: 10.1007/978-3-030-84965-8_15.
(19) Vaccaro, A.; Kaplan Dor, Y.; Nambara, K.; Pollina, E. A.; Lin, C.; Greenberg, M. E.; Rogulja, D. Sleep Loss Can Cause Death through Accumulation of Reactive Oxygen Species in the Gut. *Cell* **2020**, *181* (6), 1307−1328.e15.
(20) McCord, J. M. Radical Explanations for Old Observations. *Gastroenterology* **1987**, *92* (6), 2026−2028.
(21) Homolak, J. Gastrointestinal Redox Homeostasis in Ageing. *Biogerontology* **2023**, *24* (5), 741−752, DOI: 10.1007/s10522-023-10049-8.
(22) Bischoff, S. C.; Barbara, G.; Buurman, W.; Ockhuizen, T.; Schulzke, J.-D.; Serino, M.; Tilg, H.; Watson, A.; Wells, J. M. Intestinal Permeability–a New Target for Disease Prevention and Therapy. *BMC Gastroenterol.* **2014**, *14*, 189.
(23) Bhattacharyya, A.; Chattopadhyay, R.; Mitra, S.; Crowe, S. E. Oxidative Stress: An Essential Factor in the Pathogenesis of Gastrointestinal Mucosal Diseases. *Physiol. Rev.* **2014**, *94* (2), 329−354.
(24) Circu, M. L.; Aw, T. Y. Intestinal Redox Biology and Oxidative Stress. *Semin. Cell Dev. Biol.* **2012**, *23* (7), 729−737, DOI: 10.1016/j.semcdb.2012.03.014.
(25) Knezovic, A.; Osmanovic Barilar, J.; Babic, A.; Bagaric, R.; Farkas, V.; Riederer, P.; Salkovic-Petrisic, M. Glucagon-like Peptide-1 Mediates Effects of Oral Galactose in Streptozotocin-Induced Rat Model of Sporadic Alzheimer's Disease. *Neuropharmacology* **2018**, *135*, 48−62.
(26) Salkovic-Petrisic, M.; Osmanovic-Barilar, J.; Knezovic, A.; Hoyer, S.; Mosetter, K.; Reutter, W. Long-Term Oral Galactose Treatment Prevents Cognitive Deficits in Male Wistar Rats Treated Intracerebroventricularly with Streptozotocin. *Neuropharmacology* **2014**, *77*, 68−80.
(27) Homolak, J.; Babic Perhoc, A.; Knezovic, A.; Kodvanj, I.; Virag, D.; Osmanovic Barilar, J.; Riederer, P.; Salkovic-Petrisic, M. Is Galactose a Hormetic Sugar? An Exploratory Study of the Rat Hippocampal Redox Regulatory Network. *Mol. Nutr. Food Res.* **2021**, *65* (21), No. e2100400.
(28) Homolak, J.; Babic Perhoc, A.; Knezovic, A.; Osmanovic Barilar, J.; Virag, D.; Joja, M.; Salkovic-Petrisic, M. The Effect of Acute Oral Galactose Administration on the Redox System of the Rat Small Intestine. *Antioxidants* **2022**, *11* (1), 37.
(29) Hsiao, E. Y.; McBride, S. W.; Hsien, S.; Sharon, G.; Hyde, E. R.; McCue, T.; Codelli, J. A.; Chow, J.; Reisman, S. E.; Petrosino, J. F.; Patterson, P. H.; Mazmanian, S. K. Microbiota Modulate Behavioral and Physiological Abnormalities Associated with Neurodevelopmental Disorders. *Cell* **2013**, *155* (7), 1451−1463.
(30) Luczynski, P.; McVey Neufeld, K.-A.; Oriach, C. S.; Clarke, G.; Dinan, T. G.; Cryan, J. F. Growing up in a Bubble: Using Germ-Free Animals to Assess the Influence of the Gut Microbiota on Brain and Behavior. *Int. J. Neuropsychopharmacol.* **2016**, *19* (8), No. pyw020.
(31) Needham, B. D.; Funabashi, M.; Adame, M. D.; Wang, Z.; Boktor, J. C.; Haney, J.; Wu, W.-L.; Rabut, C.; Ladinsky, M. S.; Hwang, S.-J.; Guo, Y.; Zhu, Q.; Griffiths, J. A.; Knight, R.; Bjorkman, P. J.; Shapiro, M. G.; Geschwind, D. H.; Holschneider, D. P.; Fischbach, M. A.; Mazmanian, S. K. A Gut-Derived Metabolite Alters Brain Activity and Anxiety Behaviour in Mice. *Nature* **2022**, *602* (7898), 647−653.
(32) Babic Perhoc, A.; Osmanovic Barilar, J.; Knezovic, A.; Farkas, V.; Bagaric, R.; Svarc, A.; Grünblatt, E.; Riederer, P.; Salkovic-Petrisic, M. Cognitive, Behavioral and Metabolic Effects of Oral Galactose Treatment in the Transgenic Tg2576 Mice. *Neuropharmacology* **2019**, *148*, 50−67.
(33) Carabotti, M.; Scirocco, A.; Maselli, M. A.; Severi, C. The Gut-Brain Axis: Interactions between Enteric Microbiota, Central and Enteric Nervous Systems. *Ann. Gastroenterol.* **2015**, *28* (2), 203−209.
(34) Candas, D.; Li, J. J. MnSOD in Oxidative Stress Response-Potential Regulation via Mitochondrial Protein Influx. *Antioxid. Redox Signaling* **2014**, *20* (10), 1599−1617, DOI: 10.1089/ars.2013.5305.
(35) He, L.; He, T.; Farrar, S.; Ji, L.; Liu, T.; Ma, X. Antioxidants Maintain Cellular Redox Homeostasis by Elimination of Reactive Oxygen Species. *Cell. Physiol. Biochem.* **2017**, *44* (2), 532−553, DOI: 10.1159/000485089.
(36) Ayala, A.; Muñoz, M. F.; Argüelles, S. Lipid Peroxidation: Production, Metabolism, and Signaling Mechanisms of Malondialdehyde and 4-Hydroxy-2-Nonenal. *Oxid. Med. Cell. Longevity* **2014**, *2014*, No. 360438, DOI: 10.1155/2014/360438.
(37) Demicheli, V.; Quijano, C.; Alvarez, B.; Radi, R. Inactivation and Nitration of Human Superoxide Dismutase (SOD) by Fluxes of Nitric Oxide and Superoxide. *Free Radical Biol. Med.* **2007**, *42* (9), 1359−1368.
(38) Ursini, F.; Maiorino, M.; Forman, H. J. Redox Homeostasis: The Golden Mean of Healthy Living. *Redox Biol.* **2016**, *8*, 205−215.
(39) Kim, J.-E.; Roh, Y.-J.; Choi, Y.-J.; Lee, S.-J.; Jin, Y.-J.; Song, H.-J.; Seol, A.-Y.; Son, H.-J.; Hong, J.-T.; Hwang, D.-Y. Dysbiosis of Fecal Microbiota in Tg2576 Mice for Alzheimer's Disease during Pathological Constipation. *Int. J. Mol. Sci.* **2022**, *23* (23), 14928.
(40) Sadigh-Eteghad, S.; Majdi, A.; McCann, S. K.; Mahmoudi, J.; Vafaee, M. S.; Macleod, M. R. D-Galactose-Induced Brain Ageing Model: A Systematic Review and Meta-Analysis on Cognitive Outcomes and Oxidative Stress Indices. *PLoS One* **2017**, *12* (8), No. e0184122.
(41) Shwe, T.; Pratchayasakul, W.; Chattipakorn, N.; Chattipakorn, S. C. Role of D-Galactose-Induced Brain Aging and Its Potential Used for Therapeutic Interventions. *Exp. Gerontol.* **2018**, *101*, 13−36.
(42) Kim, D.-Y.; Jung, D.-H.; Song, E.-J.; Jang, A.-R.; Park, J.-Y.; Ahn, J.-H.; Lee, T.-S.; Kim, Y.-J.; Lee, Y.-J.; Seo, I.-S.; Kim, H.-E.; Ryu, E.-J.; Sim, J.; Park, J.-H. D-Galactose Intake Alleviates Atopic Dermatitis in Mice by Modulating Intestinal Microbiota. *Front. Nutr.* **2022**, *9*, No. 895837.
(43) Homolak, J.; Babic Perhoc, A.; Virag, D.; Knezovic, A.; Osmanovic Barilar, J.; Salkovic-Petrisic, M. D-Galactose Might Protect against Ionizing Radiation by Stimulating Oxidative Metabolism and Modulating Redox Homeostasis. *J. Radiat. Res.* **2023**, *64* (4), 743−745.
(44) Homolak, J.; Babić Perhoč, A.; Virag, D.; Knezovic, A.; Osmanovic, J.; Salkovic-Petrisic, M.D-Galactose Might Mediate Some of the Skeletal Muscle Hypertrophy-Promoting Effects of Milk - a Nutrient to Consider for Sarcopenia? *Preprint* 2023 DOI: 10.13140/RG.2.2.25134.59205.
(45) Budni, J.; Pacheco, R.; da Silva, S.; Garcez, M. L.; Mina, F.; Bellettini-Santos, T.; de Medeiros, J.; Voss, B. C.; Steckert, A. V.; da Silva Valvassori, S.; Quevedo, J. Oral Administration of D-Galactose Induces Cognitive Impairments and Oxidative Damage in Rats. *Behav. Brain Res.* **2016**, *302*, 35−43, DOI: 10.1016/j.bbr.2015.12.041.
(46) Budni, J.; Garcez, M. L.; Mina, F.; Bellettini-Santos, T.; da Silva, S.; da Luz, A. P.; Schiavo, G. L.; Batista-Silva, H.; Scaini, G.; Streck, E. L.; Quevedo, J. The Oral Administration of D-Galactose Induces Abnormalities within the Mitochondrial Respiratory Chain in the Brain of Rats. *Metab. Brain Dis.* **2017**, *32* (3), 811−817, DOI: 10.1007/s11011-017-9972-9.
(47) Chogtu, B.; Arivazhahan, A.; Kunder, S. K.; Tilak, A.; Sori, R.; Tripathy, A. Evaluation of Acute and Chronic Effects of D-Galactose

on Memory and Learning in Wistar Rats. *Clin. Psychopharmacol. Neurosci.* **2018**, *16* (2), 153−160, DOI: 10.9758/cpn.2018.16.2.153.
(48) Zhu, T.; Wang, Z.; He, J.; Zhang, X.; Zhu, C.; Zhang, S.; Li, Y.; Fan, S. D-Galactose Protects the Intestine from Ionizing Radiation-Induced Injury by Altering the Gut Microbiome. *J. Radiat. Res.* **2022**, *63* (6), 805−816.
(49) Salkovic-Petrisic, M. Oral Galactose Provides a Different Approach to Incretin-Based Therapy of Alzheimer's Disease. *J. Neurol. Neuromed.* **2018**, *3* (4), 101−107.
(50) Circu, M. L.; Aw, T. Y. Redox Biology of the Intestine. *Free Radical Res.* **2011**, *45* (11−12), 1245−1266.
(51) Jones, R. M.; Neish, A. S. Redox Signaling Mediated by the Gut Microbiota. *Free Radical Biol. Med.* **2017**, *105*, 41−47.
(52) Million, M.; Tidjani Alou, M.; Khelaifia, S.; Bachar, D.; Lagier, J.-C.; Dione, N.; Brah, S.; Hugon, P.; Lombard, V.; Armougom, F.; Fromonot, J.; Robert, C.; Michelle, C.; Diallo, A.; Fabre, A.; Guieu, R.; Sokhna, C.; Henrissat, B.; Parola, P.; Raoult, D. Increased Gut Redox and Depletion of Anaerobic and Methanogenic Prokaryotes in Severe Acute Malnutrition. *Sci. Rep.* **2016**, *6*, No. 26051.
(53) Pérez, S.; Taléns-Visconti, R.; Rius-Pérez, S.; Finamor, I.; Sastre, J. Redox Signaling in the Gastrointestinal Tract. *Free Radical Biol. Med.* **2017**, *104*, 75−103.
(54) Reese, A. T.; Cho, E. H.; Klitzman, B.; Nichols, S. P.; Wisniewski, N. A.; Villa, M. M.; Durand, H. K.; Jiang, S.; Midani, F. S.; Nimmagadda, S. N.; O'Connell, T. M.; Wright, J. P.; Deshusses, M. A.; David, L. A. Antibiotic-Induced Changes in the Microbiota Disrupt Redox Dynamics in the Gut. *eLife* **2018**, *7*, No. e35987.
(55) Tian, T.; Wang, Z.; Zhang, J. Pathomechanisms of Oxidative Stress in Inflammatory Bowel Disease and Potential Antioxidant Therapies. *Oxid. Med. Cell. Longevity* **2017**, *2017*, No. 4535194.
(56) Bercik, P.; Verdu, E. F.; Foster, J. A.; Macri, J.; Potter, M.; Huang, X.; Malinowski, P.; Jackson, W.; Blennerhassett, P.; Neufeld, K. A.; Lu, J.; Khan, W. I.; Corthesy-Theulaz, I.; Cherbut, C.; Bergonzelli, G. E.; Collins, S. M. Chronic Gastrointestinal Inflammation Induces Anxiety-like Behavior and Alters Central Nervous System Biochemistry in Mice. *Gastroenterology* **2010**, *139* (6), 2102−2112.
(57) Vorhees, C. V.; Williams, M. T. Morris Water Maze: Procedures for Assessing Spatial and Related Forms of Learning and Memory. *Nat. Protoc.* **2006**, *1* (2), 848−858.
(58) Deacon, R. M. J. Assessing Nest Building in Mice. *Nat. Protoc.* **2006**, *1* (3), 1117−1119.
(59) Ilyasov, I. R.; Beloborodov, V. L.; Selivanova, I. A.; Terekhov, R. P. ABTS/PP Decolorization Assay of Antioxidant Capacity Reaction Pathways. *Int. J. Mol. Sci.* **2020**, *21* (3), 1131.
(60) Dávalos, A.; Gómez-Cordovés, C.; Bartolomé, B. Extending Applicability of the Oxygen Radical Absorbance Capacity (ORAC-Fluorescein) Assay. *J. Agric. Food Chem.* **2004**, *52* (1), 48−54.
(61) Homolak, J.; Kodvanj, I.; Babic Perhoc, A.; Virag, D.; Knezovic, A.; Osmanovic Barilar, J.; Riederer, P.; Salkovic-Petrisic, M. Nitrocellulose Redox Permanganometry: A Simple Method for Reductive Capacity Assessment. *MethodsX* **2022**, *9*, No. 101611.
(62) Hadwan, M. H. Simple Spectrophotometric Assay for Measuring Catalase Activity in Biological Tissues. *BMC Biochem.* **2018**, *19* (1), 7.
(63) Homolak, J. In Vitro Analysis of Catalase and Superoxide Dismutase Mimetic Properties of Blue Tattoo Ink. *Free Radical Res.* **2022**, *56* (5−6), 343−357.
(64) Homolak, J.; Joja, M.; Grabaric, G.; Schiatti, E.; Virag, D.; Perhoc, A. B.; Knezovic, A.; Barilar, J. O.; Salkovic-Petrisic, M. The Absence of Gastrointestinal Redox Dyshomeostasis in the Brain-First Rat Model of Parkinson's Disease Induced by Bilateral Intrastriatal 6-Hydroxydopamine. *bioRxiv* **2022**, No. 2022-08, DOI: 10.1101/2022.08.22.504759.
(65) Homolak, J. The Effect of a Color Tattoo on the Local Skin Redox Regulatory Network: An N-of-1 Study. *Free Radical Res.* **2021**, *55* (3), 221−229.
(66) Ma, X.; Deng, D.; Chen, W.; Ma, X.; Deng, D.; Chen, W. *Inhibitors and Activators of SOD, GSH-Px, and CAT*; IntechOpen, 2017 DOI: 10.5772/65936.
(67) Marklund, S.; Marklund, G. Involvement of the Superoxide Anion Radical in the Autoxidation of Pyrogallol and a Convenient Assay for Superoxide Dismutase. *Eur. J. Biochem.* **1974**, *47* (3), 469−474.
(68) Li, X. Improved Pyrogallol Autoxidation Method: A Reliable and Cheap Superoxide-Scavenging Assay Suitable for All Antioxidants. *J. Agric. Food Chem.* **2012**, *60* (25), 6418−6424.
(69) Anderson, M. E. Determination of Glutathione and Glutathione Disulfide in Biological Samples. *Methods Enzymol.* **1985**, *113*, 548−555.
(70) De Leon, J. A.; Borges, C. R. Evaluation of Oxidative Stress in Biological Samples Using the Thiobarbituric Acid Reactive Substances Assay. *J. Visualized Exp.* **2020**, *12* (159), No. e61122, DOI: 10.3791/61122.
(71) Percie du Sert, N.; Ahluwalia, A.; Alam, S.; Avey, M. T.; Baker, M.; Browne, W. J.; Clark, A.; Cuthill, I. C.; Dirnagl, U.; Emerson, M.; Garner, P.; Holgate, S. T.; Howells, D. W.; Hurst, V.; Karp, N. A.; Lazic, S. E.; Lidster, K.; MacCallum, C. J.; Macleod, M.; Pearl, E. J.; Petersen, O. H.; Rawle, F.; Reynolds, P.; Rooney, K.; Sena, E. S.; Silberberg, S. D.; Steckler, T.; Würbel, H. Reporting Animal Research: Explanation and Elaboration for the ARRIVE Guidelines 2.0. *PLoS Biol.* **2020**, *18* (7), No. e3000411.
(72) Amrhein, V.; Korner-Nievergelt, F.; Roth, T. The Earth Is Flat ($p > 0.05$): Significance Thresholds and the Crisis of Unreplicable Research. *PeerJ* **2017**, *5*, No. e3544.
(73) Strobl, C.; Boulesteix, A.-L.; Zeileis, A.; Hothorn, T. Bias in Random Forest Variable Importance Measures: Illustrations, Sources and a Solution. *BMC Bioinf.* **2007**, *8*, 25.